

SHORT THESIS FOR THE DEGREE OF DOCTOR OF PHILOSOPHY (PhD)

Investigation of the permeability barrier in healthy and inflamed skin

Title

by Barbara Retzlerné Medgyesi

Supervisor: Andrea Szegedi, PhD, DSc



UNIVERSITY OF DEBRECEN  
DOCTORAL SCHOOL OF GYULA PETRÁNYI CLINICAL IMMUNOLOGY AND  
ALLERGOLOGY

DEBRECEN, 2023

Investigation of the skin immune system in health and inflammation

By Barbara Retzlerné Medgyesi, Medical biotechnologist (MSc degree)

Supervisor: Andrea Szegedi, PhD, DSc

Gyula Petrányi Doctoral School of Allergy and Clinical Immunology, University of Debrecen

Head of the **Defense Committee:**

Attila Bácsi, PhD, DSc

Reviewers:

Ágnes Kinyó, PhD

Edit Kapitányiné Mikó, PhD

Members of the Defense Committee:

Zsuzsanna Bata-Csörgő, PhD, DSc

Árpád Lányi, PhD

The PhD Defense takes place at the Lecture Hall of the Department of Dermatology, Faculty of Medicine, University of Debrecen, 19<sup>th</sup> June 2023, 13 pm

## INTRODUCTION

Our skin is one of the largest organs in the human body with its 1.8 m<sup>2</sup> surface. It has many important functions, contributing to the protection of the human body, its proper functioning and its homeostasis. The elements of the skin's immune and permeability barrier play an important role in these functions.

Anatomical and histological composition of the healthy skin is different on sebaceous gland-rich (SGR), apocrine gland-rich (AGR) and gland-poor (GP) skin regions. This is due to the different thickness of the stratum corneum and to the varying number of sebaceous, eccrin and apocrine glands, resulting in diverse chemical milieu on the skin surface. According to the investigations of the last decade, in parallel with the diversity of the chemical milieu, the skin microbiom also differs in the distinct skin areas. Moreover, previous results of our research group revealed that significant differences exist in the expression pattern and activity of the skin immune system between the different healthy skin regions. We demonstrated significant differences in the number and activity immune cells (DCs, T cells) of SGR, AGR, and GP skin and highlighted that the SGR and AGR regions are characterized by a non-inflammatory IL-17 / IL-10 environment with elevated levels of IL-17 related chemokines and AMPs. However, so far no one has investigated whether, similarly to the immunological barrier, the permeability barrier also differs in the three healthy skin regions. The SC layer itself and the tight junctions (TJ) in the SG layer are the two main components of the skin's permeability barrier (physico-chemical barrier), which provide protection against external environmental factors and prevent the invasion of various pathogens into the skin. They also play a role in controlling transepidermal water loss keeping the skin properly hydrated. In the research underlying the first part of my dissertation, we investigated the main elements of the permeability barrier in the three healthy skin regions: the stratum corneum elements involved in cornified envelope formation, corneocyte desquamation and (corneo)desmosome organisation, and tight junction molecules. First, I will summarise our results in this topic.

Rosacea mainly affects the sebaceous gland rich (SGR) skin areas. This immune mediated skin disease is located on the central part of the face, where it causes skin dryness, elevated pH and TEWL together with increased dehydration, suggesting the damage of the permeability barrier. We aimed to investigate the permeability barrier alterations of rosacea skin, I will present this topic in the second part of my PhD project.

## **OBJECTIVES**

### **1.Examination of the permeability barrier of healthy skin**

Previous investigations has revealed that the microbial composition, chemical milieu, and immune tuning show prominent differences on topographically distinct healthy skin areas. According to our research, the antimicrobial barrier of the skin can not be considered uniform either, since we detected significant differences in the AMP expression of the SGR, AGR and GP regions. As the antimicrobial and permeability barriers of the skin are closely related, we aimed to study the gene and protein expression of the two main elements of the permeability barrier, the SC and the TJ layer, and to study their organization in different healthy (SGR, GP and AGR) skin regions.

In our research, we aimed to perform the following investigations in the three healthy skin regions:

1. Investigation of transepidermal water loss (TEWL) to study the function of permeability barrier (functional studies)
2. Analysis of the SC molecules at the gene [RNA Seq, Quantitative Real-Time Polymerase Chain Reaction, (QRT-PCR)] and the protein [Immunohistochemistry (IHC)] levels
  - a, CE intracellular structure molecules
  - b, Molecules involved in corneocyte desquamation and the formation of intercellular lipid lamellae
  - c, Components involved in the organization of (corneo)desmosome
3. Investigation of TJ molecules at the gene (QRT-PCR) and the protein (IHC) levels
4. Examination of the organization of the above-mentioned molecules by confocal microscopy

### **2. Examination of permeability barrier rosacea**

Since rosacea, a chronic disease of the sebaceous gland-rich facial skin, is characterized by severe skin dryness, elevated pH and TEWL suggesting permeability barrier damage, we aimed to investigate the permeability barrier at the molecular level in rosacea, and compared to SGR skin.

1. We aimed to explore the differences in gene expression patterns by whole transcriptome analysis

2. To study the SC and TJ barrier molecules at the gene (QRT-PCR) and the protein (IHC) levels:
  - a, Molecules involved in CE formation
  - b, Molecules involved in the formation of intercellular lipid lamellae
  - c, (Corneo) desmosome components and enzymes responsible for the corneocyte's desquamation and cross-linking
  - d, TJ components
  - e, AMPs involved in the formation of the immunological barrier
3. We further aimed to compare the characteristics of the rosacea and AD permeability barrier by IF methods.

## **MATERIALS AND METHODS**

### **Collection of samples and sample preparation**

#### *Skin Biopsies*

Skin punch biopsies (0.5-1 cm<sup>2</sup>) were taken from patients suffering from immune-mediated skin diseases and from normal skin of healthy individuals. In our first investigation we collected biopsy samples from different skin regions of healthy individuals who undergone plastic surgery: 8-8-8 samples from sebaceous gland-rich (SGR), gland-poor (GP) and apocrine gland-rich (AGR) skin regions. For our second investigation we collected samples from the lesional (facial) skin of 8 patients with papulopustular rosacea (PPR) and from the SGR skin of 8 healthy volunteers. The study was approved by the Hungarian Medical Research Council and the local Ethics Committee of University of Debrecen, Hungary.

The donors underwent surgery after obtaining written, informed consent, according to the Declaration of Helsinki principles. All biopsies were cut into 2 pieces. For immunohistochemistry (IHC) and immunofluorescence (IF) investigations half of the samples were embedded into paraffin after formalin fixation whereas the remaining parts were placed in RNAlater and stored at -80°C until QRT-PCR investigation. After hematoxylin-eosin staining the embedded samples were sorted according to the number of sebaceous and apocrine glands. Samples were defined as GP skin when containing  $n \leq 1$  sebaceous glands and as SGR skin when containing  $n \geq 3$  sebaceous glands and AGR skin containing glands  $n \leq 2$  in the field of view on 10x magnification in the microscope.

### **RNA isolation, Reverse Transcription**

After removing the subcutis (subcutaneous adipose tissue) from the samples stored in the RNA later, we homogenized it in tri-reagens solution with tissue lyser after using autoclaved steel balls. After homogenization, RNA was isolated from skin samples according to the trizol protocol. The quality of the RNA was determined with a Agilent 2100 bioanalyzer. For the QRT-PCR, 1 $\mu$ g of RNA was transcribed into cDNA (complementary DNA), preceded by DNase I enzyme treatment to prevent possible genomic DNA contamination. We performed the cDNA synthesis by using the High Capacity cDNA Archive Kit according to the instructions of the manufacturer.

### **Quantitative- Real-Time PCR**

The QRT-PCR measurements were carried out in triplicate using pre-designed FAM-MGB assays as well as TaqMan® Gene Expression Master Mix. All measurements were performed with a ABI PRISM® 7000 System. Relative mRNA levels of target genes were calculated using the comparative  $\Delta\Delta$ CT methods normalized to the expression of PPIA mRNA.

### **RNA sequencing and (RNAseq) analysis**

cDNA library for RNASeq was generated from 1mg total RNA using TruSeq RNA Sample Preparation Kit according to the manufacturer's protocol. Poly-A-terminal RNAs were purified with oligodT-conjugated magnetic beads and fragmented at 94 ° C for 8 minutes. We used random primers and SuperScript II reverse transcriptase enzymes to transcribe the single-stranded cDNA. The next step was the synthesis of the second strand of the cDNA. After repairing the double-stranded cDNA ends and adenylating the 3' ends, the Illumina index adapters were ligated to the sample. The adapter-ligated cDNA fragments were then amplified by PCR. Fragment size distribution and molarity of libraries were checked on an Agilent Bioanalyzer DNA1000 chip. Concentrations of RNASeq libraries were set to 10nM and 5 libraries were pooled together before sequencing. A single reading 50bp sequencing run was performed on an Illumina HiScan SQ instrument and 16-18 million readings per sample were obtained. The CASAVA software was used for pass filtering and demultiplexing process. Sequenced readings were aligned to Human Genome v19 using TopHat and Cufflinks algorithms and bam files were generated. The StrandNGS software was used for further statistical analysis. Bam files were imported and normalized using DESeq algorithm. To identify statistically significant gene expression patterns between the different conditions, the non-parametric Wilcoxon Mann-Whitney test was used. Library preparations, sequencing

and data analysis were performed by Dr. Szilárd Póliska in the Genomic Medicine and Bioinformatics Core Facility of University of Debrecen. RNASeq data samples (SGR1-SGR6) have been previously published and deposited to the Sequence Read Archive (SRA) database (<https://www.ncbi.nlm.nih.gov/sra>) under accession number PRJNA421246. While samples SGR7, SGR8 and PPR1-PPR8 are available in the Sequence Read Archive database under reference number PRJNA592080.

### **Pathway analyses**

To identify the function of the aforementioned differentially expressed genes (DEGs), multiple bioinformatics analyses were performed by Cytoscape ClueGO bioinformatics tool using Gene Ontology (GO) Biological Process (BP), GO Immune System Process (ISP), and Molecular Function (MF); Kyoto Encyclopedia of Genes and Genomes (KEEG), Reactome Pathways; and Reactome Reactions databases. First, to identify the general biological function of DEGs, we performed a pathway enrichment analysis on all DEGs with  $FC \geq 1,5$ . To reveal the significantly enriched ( $P < 0,05$ ) terms and pathways, the following criterion was applied: all terms should have contained at least 50 genes from our input gene set. Then, we performed a second, stricter pathway enrichment analysis to find out the function of barrier-related significant DEGs with  $FC \geq 1,5$  in more detail; thus, a different analytical approach was applied. Up- and downregulated DEGs were subjected as two different clusters to a more detailed pathway enrichment analysis by ClueGO. According to the fact that most DEGs were upregulated (approximately 61%), the criteria of the analysis were different in the cases of up- and downregulated gene sets. Regarding the cluster of upregulated genes, terms should have contained at least 30 genes from our input gene set and at least 20% of all genes characteristic to each term, whereas the cluster of down- regulated genes required at least 18 genes from our input gene set and at least 12% of all genes characteristic to each term. This approach allowed us not only to reveal significantly enriched specific terms and pathways but also made us capable of easily distinguishing and visualizing up- and downregulated DEGs belonging to each terms.

### **Immunohistochemistry (IHC), immunofluorescent (IF) and routine staining**

For IHC analyses, paraffin-embedded sections from diseased and healthy skin tissues were deparaffinized, than, as a next step rehydration and heat-induced antigen retrieval was performed. Section were also preprocessed with 3%  $H_2O_2$  for 15 minutes to inhibit endogenous peroxidases. Sections were stained with primary anti-human antibodies.

Subsequently, anti-mouse/rabbit peroxidase-conjugated secondary antibodies were employed. The samples were washed before and after incubating for 5 minutes, 3 times in each step, staining was detected with the ImmPACT™ NovaRED™ Kit or 33'-Diaminobenzidine-t (DAB). Methylene green background staining was also applied to the sections. As a final step in the process, the stained sections were covered with glass coverslip after dehydration. The proteins of interest were detected parallelly on all sections in order to make the protein expressions comparable during the evaluation.

Positive, Ig and isotype controls were also used to normalize the staining of proteins. IF staining, similar to IHC staining, was performed on deparaffinized sections and the experimental procedure was similar until the application of the secondary antibody. After incubation with the primary antibodies, secondary antibodies were used. The haematoxylin-eosin stainings were performed to determine the number of the sebaceous glands.

### **Whole-slide imaging**

The slides were digitalized using a Pannoramic SCAN digital slide scanner with a Zeiss plan-apochromatic objective and Hitachi 3CCD progressive scan color camera. Immunostainings were analyzed with the Pannoramic Viewer software 1.15.2, using the HistoQuant applications. Regions of interest (ROIs) (n=20/slide) were selected and then the Field Area [FA (mm<sup>2</sup>)] and the Mask Area [MA (mm<sup>2</sup>)] were measured by the software. The FA shows the whole area of the ROI and the MA represents the positive area. The MA/FA values were counted for all ROIs.

### **Mesasurement of Transepidermal Water Loss**

Measurements were performed under standardized laboratory conditions at a temperature of 22–25°C and a humidity level of 40–60% in healthy individuals (n=30). Individuals were allowed to adapt to room conditions for at least 15 min before the measurements. Transepidermal water loss (TEWL) measurements (g/hm<sup>2</sup>) were carried out with the Tewameter TM300 on the flexural forearm (representing GP region), axilla (representing AGR area), and forehead (representing SGR region). Measurements were performed in triplicate for 30s each.

## **Confocal Microscopy**

For confocal microscopy, four 40 µm thick skin specimens were assessed from each sample group. Skin specimens were deparaffinised, and heat-induced antigen retrieval was performed. Incubations with the primary and secondary antibodies were performed on free-floating specimens for 48 hours at 4 °C and 2 hours at room temperature, respectively. Finally, specimens were placed on slides and mounted with VECTASHIELD® HardSet™ Antifade Mounting Medium with DAPI. Imaging of immunostained samples was performed using an Olympus FV3000 confocal instrument with a 60x oil immersion lens. Predetermined settings (laser power, confocal aperture and gain, detector parameters) were identical for all samples.

A series of 1 µm thick optical sections with 0.5 µm separation in the Z-axis were acquired. Images for figures were processed using the Adobe Photoshop CS5 software. Line profiles for the green and red channels were measured and plotted using the FIJI image analysis package. Due to the variable length of the ROIs only the first 50 micrometers (starting from stratum granulosum) were compared. The regularity of the DSG1 and CLDN immunostaining was analysed by measuring the distance between two adjacent immunostained dots along the cell membrane cross-section (a closed line around a DAPI stained nucleus in the region of stratum granulosum). For a given skin type, 100 inter-dot distances were measured.

## **Statistical analyses**

To assess the distribution of the data, the Kolmogorov–Smirnov test was used. Because of their normal distribution, we determined mean with corresponding 95% confidence interval. P-values <0.05 were considered statistically significant (\*p < 0.05; \*\*p < 0.01; \*\*\*p < 0.001). Statistical analyses were performed using the GraphPad Prism software version 6.

## **RESULTS**

### **I. Investigation of the permeability barrier of the healthy skin**

#### ***I.1. Measurement of TEWL in different skin regions***

As a first step, in order to study barrier function, we performed transepidermal water loss (TEWL) measurements in 30 healthy people. The TEWL measurements were performed in the 3 skin regions (SGR, AGR and GP skin regions). The TEWL of SGR skin was measured

on the forehead and face, in the axilla as the AGR skin, and on the forearm and leg as the GP skin. We found significantly higher TEWL levels in the SGR and AGR regions compared to GP areas, indicating differences in the barrier function among the three skin regions. Differences were more prominent between the AGR and GP areas (6.89 fold increase) than in SGR versus GP areas (1.57 fold increase).

### ***1.2. Investigation of the expression of Cornified envelope intracellular structural molecules in different skin regions***

Since we detected significant differences among the permeability barrier of the three skin regions, we aimed to study the most important molecules of the permeability barrier at the molecular level as well.

We were the first to perform gene-level analyses of the molecules involved in the formation of CE among the SC components involved in the barrier function by QRT-PCR method, and then we used the quantitative IHC method for our protein-level studies.

No significant differences were detected among the three skin regions in the mRNA and protein expression of molecules taking part in cornified envelope formation, including KRT1, KRT10, LCE1D, LCE1F, SPRR1A, SPRR2A, TGM1, and TGM5.

### ***1.3. Investigation of the expression of KLK proteases and the ABCA12 lipid transporter in different skin regions***

We investigated the expression of KLK5 and KLK7 enzymes, which play crucial roles in corneocyte desquamation, by QRT-PCR method. Based on our results, KLK5 and KLK7 molecules were significantly upregulated at the mRNA level in SGR and AGR areas compared with GP regions. Protein levels for both enzymes in the interfollicular and follicular epidermis were similar in the three sample groups. However, IHC revealed stronger positive staining for KLK5 and KLK7 in the apocrine and sebaceous glands of AGR and SGR regions, resulting in substantial differences between gland-rich and GP skin regions.

In addition to these enzymes, we examined ABCA12, which is a molecule involved in the formation of intercellular lipid lamellae. Regarding this transporter molecule, its gene expression levels were significantly higher in both SGR and AGR regions versus GP areas. Moreover, in AGR epidermis, ABCA12 transporter was slightly but significantly upregulated at the protein level compared with GP skin.

#### ***1.4. Investigation of the corneo(desmosome) and tight junction components in different skin regions***

Concerning the (corneo)desmosome components, mRNA expression of CDH1, CDSN, DSC1, DSG1, and PKP1 did not differ significantly among the 3 healthy skin regions. In contrast, at the protein level, the expression of DSG1 and CDSN molecules were different in the skin areas.

At the protein level, DSG1 was significantly downregulated in both SGR and AGR skin, and the level of CDSN was significantly decreased in SGR compared with GP skin. Regarding the TJ components, at the gen expression level, CLDN1 was significantly increased in AGR and CLDN23 was upregulated in SGR regions compared to GP skin. In contrast, similar mRNA levels were detected for CLDN16, CDH1, and OCLN in all 3 regions.

Gene level analysis of TJ components showed that CLDN1 expression was significantly increased in AGR skin regions compared to GP regions, while CLDN23 showed an increase in SGR skin regions compared to GP skin regions. However, similar mRNA levels were observed for CLDN16, CDH1 and OCLN in all three regions. However, our protein level studies showed that CLDN1 molecule expression was significantly decreased in the AGR region compared to the GP region, and OCLN levels were lower in both SGR and AGR regions than in GP skin.

#### ***1.5. Investigating the organization of cell junctions on different skin regions***

Next, we examined whether the decrease in protein expression of (corneo)desmosome and TJ molecules in the AGR and SGR regions is associated with altered organization of these cell junction structures. This question was investigated using confocal microscopy. DSG1 and CDSN molecules, representing (corneo)desmosomes, were detected by double immunofluorescent staining. As expected, the CDSN molecule was strongly expressed in the SG layer in GP skin areas, but was not detected in the deeper layers. DSG1 protein was also mostly localized in the stratum granulosum layer, with decreasing trend towards the basal epidermal layers. For both proteins, we observed strong staining and co-localization (representing corneodesmosome formation) in the 1-2 cell layer of the stratum granulosum. Since we were also interested in the organization level of corneodesmosomes, we measured the distances between two adjacent immunostained DSG1 dots in the cross-section of the cell membrane in the SG layer. We found that the structures represented by DSG1 were regularly located around the keratinocytes in the GP epidermis. In contrast to the GP region, an expansion of CDSN expression towards the SS was observed in the SGR and AGR regions,

moreover DSG1 expression could be detected both the SG and deeper layers in these regions. Consequently, co-localization of CDSN and DSG1 was less dense and spread over a wider range of cell layers in the SGR and AGR regions than in the GP regions. Furthermore, the spatial distribution of corneodesmosomes (represented by DSG1 positive dots) was less organized, showing an irregular distribution in the SGR skin, even more in the AGR regions. The IF staining of the CLDN1 molecules representing TJ structures in the GP region was strongest region in the SG, and the distribution of CLDN1 dots was highly regular in this skin regions. In contrast in the SGR and AGR regions, the CLDN1 immunostaining pattern was widened towards the SS, and CLDN1 dots were irregularly distributed in the SGR samples, and even more irregularly distributed in the granular layer of the AGR skin.

## **II. Examination of the rosacea skin barrier**

### ***II.1. Heatmap, Principal Component Analysis (PCA)***

To identify differences in gene expression patterns between SGR and PPR skin, RNA sequence analysis was performed on lysates from 8 healthy SGR and 8 PPR donor skin samples. Using the results of the sequencing, we created a heatmap and a Principal Component Analysis (PCA) plot using StrandNGS software. These plots help to visualise the differences between the two groups. The difference in the gene expression profile of PPR and SGR skin samples is clearly observed in the software generated heat map. The PCA graph also illustrates the difference between the two studied groups. The dots in the PCA plot represent a skin sample from each donor, where the colours represent the PPR and SGR skin regions (red: PPR, blue: SGR). The distances between the dots indicate the extent of the differences between the gene expression profiles of the samples. The figure clearly shows that the different coloured dots are arranged in two groups, and the distance between the red and blue group is more significant than the distances within the solid-coloured group. In the PCA plot, it can also be observed that points belonging to the same region are generally relatively small, while in other regions the same colour points are in a relatively higher distance from each other. The Mann-Whitney non-parametric statistical test ( $p < 0.05$ ) was used to determine differences in gene expression profiles between PPR and SGP samples. The statistical threshold was defined as a fold change (FC) of at least 1.5-fold between the 2 sample groups in the mean expression of each gene, with statistical significance of  $p < 0.05$ . Among differentially expressed genes (DEGs), 3133 genes were expressed at higher levels in PPR compared to SGR skin samples, while 2003 genes were expressed at lower levels.

## ***II.2. Pathway analysis 1***

To identify the function of the DEGs, several bioinformatic analyses were performed using the bioinformatics tool Cytoscape ClueGO. First, to identify the general biological function of DEGs, we performed a pathway enrichment analysis on all DEGs with  $FC \geq 1,5$ . To identify the significantly enriched ( $p \leq 0,05$ ) terms and/or pathways with global biological functions, we used the criterion that all pathways contain at least 50 genes from the input gene list. Based on this, the ClueGO application identified 1239 statistically significant enriched terms. Not surprisingly, the identified terms were mostly involved in cellular/metabolic functions (e.g., ion transport, lipid biosynthetic process, and transferase activity) and innate (e.g., response to external stimulus, response to stress, cytokine secretion, defense response to bacterium, NOD-like receptor signaling pathway, and complement activation) and adaptive (e.g., T-cell activation, leukocyte migration, TNF production, IFN-gamma production, and chemokine signaling pathway) immune mechanisms. In addition, genes involved in neuronal functions (e.g. development of the nervous system) and vascularisation (e.g. regulation of vascular development, angiogenesis) were also found to differ. For us, the most important information was that 24 terms (e.g. epithelial development, epithelial morphogenesis, epithelial cell differentiation and proliferation) with skin barrier-related functions were also involved.

## ***II.3. Pathway analysis 2***

As a continuation of our bioinformatic studies, we performed another bioinformatic analysis to determine more specific functions of DEGs. Compared to the previous analysis, a more stricter analytical approach was applied, the up- and downregulated DEGs were analyzed as two different clusters by ClueGO application. This analytical approach revealed 426 significantly enriched terms and/or pathways and most of them (291) belonged to innate and adaptive immune mechanisms (e.g., T helper type [Th] 17 cell differentiation, toll- like receptor cascades, T-cell selection, and neutrophil migration). In addition, several terms were involved in cellular and metabolic functions (63 terms; e.g., transport along microtubule, exocytosis of specific granule membrane proteins, and response to cAMP) and took part in vascularization (2 terms; positive regulation of vasculature development and positive regulation of angiogenesis) and the nervous system (21 terms; e.g., axonogenesis, glial cell differentiation, and axon guidance) were differentially expressed. What was really relevant for us was that in our analysis we identified 15 pathways that are associated with a barrier

function of the skin (e.g. keratinization, cornification and tight junction). In our further studies we focused on these pathways.

#### ***II.4. RT-QPCR and IHC validation confirm the significant alterations in the major skin barrier components in PPR***

The RNA sequencing results revealed that the permeability barrier of rosacea skin is significantly different from that of healthy sebaceous skin. In order to better understand the differences between the permeability barrier of PPR and healthy SGR skin, gene expression of the main groups of permeability barrier molecules was validated by QRT-PCR. This method allows us to "back-check" the differences in gene expression patterns obtained during sequencing.

Based on the results of our previous analyses and literature data, we have selected the most important groups and molecules involved in the skin permeability barrier function: (i) in the cornified envelope formation (FLG, KRT1, KRT10, LCE1D, LCE1F, LOR, SPRR1A, SPRR2A, TGM1, TGM3, and TGM5), (ii) in the intercellular lipid lamellae formation (ABCA12), (iii) in the desmosome organization (CDH1, corneodesmosin [CDSN], desmoglein 1 [DSG1], DSC1, and PKP1), (iv) in the corneocyte desquamation (kallikrein [KLK]5, KLK7, and KLK14), (v) molecules involved in tight junction formation (CLDN1, CLDN16, CLDN23, and OCLN), (vi) molecules involved in barrier alarmin function (KRT6, KRT16, and KRT17), but in addition some (vii) important AMPs were also investigated (S100A7, S100A8, S100A9, DEFB4B, LCN2, and cathelicidin). Some representatives of the above mentioned molecular groups were also investigated by IHC coupled with an image analysis, thus providing insight into their expression at the protein level.

##### ***II.4.1. Cornified envelope formation***

First the molecules involved in the formation of CE were analysed by QRT-PCR, which showed that the genes were similarly expressed as found by RNA sequencing. Our results showed that most of the investigated barrier structure molecules (KRT1, KRT10, FLG, LOR, LCE1D and LCE1F) were downregulated, while SPRR1A and SPRR2A were upregulated in PPR samples compared to healthy controls. The differences were statistically significant in all cases except for the two late cornified envelope molecules (LCE1D, LCE1F) and the SPRR1A molecule. Enzymes crucial for peptide cross-linking (TGM1, TGM3 and TGM5) were expressed at similar levels in PPR and SGR samples. Following the gene level

determinations, further tests were carried out for some selected CE components. Since we considered it important to confirm the different expression of these molecules between the two skin regions at the protein level, we performed IHC staining. Our studies found that LOR and KRT1 protein expression was significantly lower in PPR than SGR skin, while FLG protein was similarly expressed in both sample groups. Among the enzymes, TGM5 molecule staining was performed, and the protein level showed no significant difference between PPR and healthy SGR skin samples.

#### ***II.4.2. Intercellular lipid lamellae formation***

Among molecules with a pivotal role in composing intercellular lipid lamellae, the gene expression level of ABCA12 was assessed by RT-qPCR in PPR and healthy SGR samples. According to our results, ABCA12 molecule was expressed in a significantly lower mRNA level in rosacea compared to controls.

#### ***II.4.3 Desmosome organization***

The gene expression levels of desmosome components (DSG1, DSC1, CDSN, PKP1, and CDH1) were examined by RT-qPCR. We found that all investigated molecules, except CDSN, were expressed at significantly lower levels in PPR samples compared to SGR. No significant difference in CDSN mRNA levels was detected between the two sample groups. Subsequently, two selected junction components (DSG1, CDSN) were also examined at the protein level by IHC staining. Our results showed that DSG1, similarly to its expression at the mRNA level, was expressed in a significantly lower protein level in PPR compared to SGR samples. Another important protein involved in desmosome organization, CDSN, was similarly expressed in both skin samples, confirming our findings at the mRNA level, where we also found no significant differences between the two sample groups.

#### ***II.4.4. Corneocyte desquamation***

In the next study, the expression of enzymes (KLK5, KLK7 and KLK14), playing key role in desquamation, were investigated in the two groups. At the mRNA level, we found that the expression levels of KLK5, KLK7 and KLK14 were very similar in PPR and SGR skin samples.

#### ***II.4.5. TJ formation***

Next, we examined the gene expression levels of CLDN1, CLDN16, CLDN23 and OCLN in the two skin regions, and we found that they were expressed at lower levels in PPR skin samples compared to SGR. We also performed immunohistochemical analysis of the CLDN1 molecule, detecting significantly lower protein levels in PPR samples compared to SGR skin.

#### ***II.4.6. Barrier alarmins***

As a next step, we investigated the expression of KRT6, KRT16 and KRT17 molecules in the two groups, as these molecules are highly induced during epidermal barrier damage. First, the selected barrier alarmins were analyzed at the mRNA level by QRT-PCR. According to our results, gene expression levels of KRT6, KRT16 and KRT17 were significantly increased in PPR compared to SGR skin. Next, we performed the IHC staining of KRT6, which confirmed our results at the mRNA level, as while we could not detect KRT6 molecule at the protein level in sebaceous skin, we observed robust expression in PPR.

#### ***II.4.7. AMPs***

It was considered also important to investigate the expression levels of AMPs, key components involved in the immunological barrier function of the skin. First, we studied the gene expression level of S100A7, S100A8, S100A9, DEFB4B, LCN2 and CAMP using QRT-PCR. Our results showed that the expression of all investigated AMPs is significantly upregulated in PPR samples compared to healthy SGR skin. To confirm that the increased mRNA levels resulted in increased protein levels, we also measured S100A8 and LCN2 molecules by IHC. Our results revealed that both S100A8 and LCN2 protein levels are significantly higher in PPR samples compared to controls.

### ***II.5. Disrupted skin barrier features of PPR are similar to that of AD***

#### ***II.5.1. Literature search***

As barrier alterations in PPR seemed to be similar to that of lesional AD skin, we reviewed the literature on AD barrier damage and compared barrier alterations of the two disorders. According to the literature search, the skin barrier alterations were similar in PPR and AD skin compared with the respective healthy control skin (SGR and sebaceous gland poor [SGP] samples).

### ***II.5.2. Immunofluorescent staining***

As a continuation of our studies, to confirm the similarities in skin barrier changes between PPR and AD, immunofluorescent staining was performed in PPR and AD samples. IF testing was also performed on the respective control groups (SGR and GP skin samples). The results of the immunostaining showed that LOR of CE molecules, as well as key components of desmosomes and TJ (DSG1 and CLDN1) were strongly downregulated in PPR and AD samples compared to control groups.

The KRT6 barrier alarmin molecule and the S100A8 AMP protein were almost completely absent in healthy skin samples, whereas these molecules were highly expressed in PPR and AD skin samples. Based on our immunofluorescence studies, the pattern of the investigated proteins was similar in rosacea and AD.

## **DISCUSSION**

### **1. The permeability barrier of the healthy skin**

There are significant regional differences in the anatomical and physiological properties of the skin, and recent studies have shown that there are also significant differences in the microbiota composition and immune activity of distinct skin areas. We aimed to comprehensively analyse the permeability barrier of topographically different healthy skin regions using functional measurements and multiple mRNA- and protein-based methods. Our functional analysis revealed that TEWL was significantly higher in the SGR and AGR skin regions compared to GP areas, indicating that AGR and SGR regions may be associated with a weaker permeability barrier, although the TEWL values measured in the axillary region may be influenced by the high number of sweat glands. This finding was similar to the results of a study by Kleesz and colleagues, who also found higher TEWL in the SGR and AGR skin regions compared to the GP region, and the AGR skin region had the highest TEWL of the three skin regions.

Molecular analysis of intracellular structural proteins revealed no differences between the different skin areas. Although similar mRNA levels for extracellular junctions were detected in the three skin areas, significantly reduced protein expression was detected for several corneodesmosomes and TJ molecules in AGR and SGR skin regions compared to GP skin region. The facts that the differences occurred only in the expression of extracellular cell junction components and only at the protein level, suggest that extracellular proteolytic degradation rather than reduced protein production is responsible for the weakened permeability barrier in AGR and SGR skin areas.

Our hypothesis was further supported by the significantly higher expression of KLK5 and KLK7 extracellular proteases mRNA levels in AGR and SGR skin compared to the GP region.

In addition, KLKs increased at the protein level in AGR and SGR regions due to their production by the apocrine and sebaceous glands, respectively. These results are also consistent with a previous study in which higher levels of KLK were detected in sweat samples collected from the face and axilla. Since DSG1, DSC1, and CDSN are the major cleavage targets of KLK5 and KLK7, we hypothesize that these enzymes may be directly responsible for the degradation of corneodesmosomes in the SGR and AGR skin regions.

Furthermore, KLKs can also activate several enzymes involved in TJ degradation (e.g. PAR2, matrix metallo-proteases), which, at least in part, may also be responsible for TJ weakness in the SGR and AGR regions. In addition, region-specific bacteria and fungi (Propionibacterium and Malassezia on SGR; Corynebacterium, Proteobacteria, and Staphylococcus aureus on AGR skin) influence the permeability barrier by producing exogenous serine and cysteine peptidases.

The lipid transporter ABCA12 is a molecule that plays a key role in the formation of lipid lamellae. mRNA level analysis showed strong upregulation of this molecule in the SGR and AGR regions, and a significant increase in the AGR regions compared to GP at the protein level. The differences in ABCA12 expression highlight the heterogeneous nature of our skin; however, further studies are needed to confirm this.

To confirm our molecular results and to understand the organization and distribution of corneodesmosomes and TJs, we also examined different skin regions by confocal microscopy. Our results showed that (corneo)desmosomes and TJ molecules are regularly distributed in the GP region, as expected. In contrast, in the AGR and SGR regions the coupling structures were disordered.

In summary, healthy AGR and SGR skin regions are equipped with higher TEWL, enhanced presence of KLK enzymes, decreased expression of certain (corneo)desmosome and TJ proteins, and irregularly distributed corneodesmosomes and TJs compared to GP areas. These results indicate that AGR and SGR regions are the so-called weak links of our skin.

Our current results may also be clinically important, as they may explain why some acantholytic skin diseases, including pemphigus foliaceus (PF), Darier's disease (DD) and Hailey-Hailey disease (HHD), appear at a certain age and in a certain skin region. A common feature of these skin diseases is the loss of KC adhesion due to impaired

desmosome/(corneo)desmosome formation caused by mutations in DD and HHD and autoantibodies in PF. In DD and HHD, mutations in the ATP2A2 and ATP2C1 Ca<sup>2+</sup> pump genes cause damaged desmosome/(corneo)desmosome formation, and although these genes are present throughout life and in all KC, the clinical signs themselves usually appear after adolescence and almost always in the SGR/AGR areas.

We hypothesize that the genetic alterations in DD and HHD desmosomes manifest after puberty, and mostly in the SGR and AGR skin regions, because these regions are characterized by a weaker permeability barrier, which appears after puberty as a result of the adolescent microbiota shift, increased KLK enzyme levels, degradation of coupling proteins and consequently weakened desmosomes and TJs. Both the characteristic SGR/AGR localization of these diseases and their common appearance after puberty can be explained based on our results. In PF, although anti-desmoglein1 antibodies bind to desmosomes in the whole skin surface, the first and predominant clinical signs of bulla formation occur mainly on SGR areas, where the weakness of (corneo)desmosomes/TJs sensitize these regions more susceptible to disease development. Significant therapeutic consequences may also be drawn from these data. The regulation of enzymes that are likely responsible for enhanced degradation of extracellular junction molecules and, consequently, the weakened cell junctions of SGR/AGR skin areas, by locally applied inhibitors or antibiotics, may delay or obstruct the occurrence of these diseases.

In conclusion, our skin is a topographically heterogeneous, non-unified organ represented not only by regionally distinct chemical and microbial milieu, and different immune tuning, but also by distinct permeability barrier characteristics. The unique characteristics of topographically distinct skin areas have a significant impact on the pathogenesis, development and localization of established skin diseases. These data should be taken into account not only scientifically but also in therapeutic approaches.

## **2. Examination of the permeability barrier in rosacea**

Clinical features and functional studies on the affected facial skin of patients with rosacea indicate the presence of permeability barrier alterations. However, no detailed analysis of skin barrier disruption in rosacea at the molecular level has been conducted so far. In the present study, we performed a whole transcriptome analysis (RNASeq) of PPR skin samples and gene expression profiles of diseased skin were compared with that of healthy SGR skin.

An intact skin barrier is essential for maintaining homeostasis, as it protects our body from various microbes and external influences, and provides a waterproof cover. According to the literature, stratum corneum, the outermost layer of the epidermis, and tight junctions are considered the most important components of the skin permeability barrier. Molecules forming the stratum corneum can be further divided into four groups: cornified envelope formation, intercellular lipid lamellae formation, corneodesmosome organization, and corneocyte desquamation. Cornified envelope is built up from several types of intracellular structure proteins, including FLG, LOR, LCE, and SPRR proteins; envoplakin; periplakin; involucrin; and KRT filaments that are derived from keratohyalin granules. Cross-linking of these proteins is catalysed by the enzymes TGM1, TGM3 and TGM5. According to our results, FLG, LOR, KRT1, KRT10, and LCE1D molecules were significantly downregulated, whereas SPRR2A showed significantly higher expression in PPR skin compared to healthy SGR skin. We also confirmed a significant reduction of LOR and KRT1 in rosacea skin by our protein level assays. Regarding the expression of TGMs, no significant difference was detected either at mRNA or protein levels. Lipid lamellae formation is also important in the development of an intact stratum corneum layer, where lipoxygenases (ALOX12B and ALOXB3) and lipid transporters (ABCA12) play an essential role in the synthesis and transport of lipids. In our study, the ABCA12 molecule showed significantly reduced mRNA expression in PPR compared to control skin. Another component of the SC is the desmosome apparatus, which is responsible for the cell adhesion of corneocytes. Based on our findings, desmosomes are highly disrupted in PPR, as demonstrated by the significantly decreased gene expression levels of CDH1, CDSN, DSC1, DSG1, and PKP1. The significant decrease in DSG1 was also confirmed at the protein level by IHC.

In the stratum corneum, corneocytes are shed as part of an event called desquamation, which is primarily regulated by KLKs (KLK5, KLK7, and KLK14) via a pH-dependent proteolytic cascade. In our study, we detected similar gene expression levels of KLK5, KLK7, and KLK14 in lesional PPR compared with healthy skin; we did not investigate the protein levels and activities of the enzymes.

In addition to the stratum corneum, tight junctions are also key components for the integrity of the skin barrier by sealing adjacent keratinocytes in the stratum granulosum and acting as a barrier for water and solutes. Tight junctions are composed of transmembrane proteins, particularly the CLDNs and OCLN. In our study, mRNA levels for CLDN1, CLDN16, CLDN23, and OCLN were significantly decreased in PPR compared to the control group. The significant decrease in CLDN1 was confirmed at the protein level by IHC. In parallel with the

stratum corneum and tight junction components, we focused on investigating two additional groups of molecules, key barrier alarmins and AMPs, because the expression levels of these molecules are tightly connected with the level of permeability barrier structural components. In our study, all investigated barrier alarmins (KRT6A, KRT16, and KRT17) and AMPs (cathelicidin, hBD-2, LCN2, S100A7, S100A8, and S100A9) were significantly upregulated in PPR skin compared with controls. The significantly higher presence of LCN2, S100A8, and KRT6 was also confirmed at the protein level in PPR. To our knowledge, until now, only one study has investigated rosacea samples at a whole transcriptomic level. In this study, the authors focused on examining the immunological characteristics of different rosacea subtypes, and no data were published on barrier components.

In another study, Deng and colleagues investigated the expression of CE components, including KRT10, FLG and LOR mRNA in various rosacea subtypes. They also examined the expression of CLDN1 TJ protein and, similar to our results, found significantly lower gene and protein levels in rosacea compared to control samples. Regarding the mRNA levels of KRT10 and LOR, the authors of this study did not find significant differences when comparing PPR to controls, and protein levels were not assessed. The expression of KLK5 in rosacea has been studied previously by another workgroup, and its mRNA and protein levels were demonstrated to be significantly increased, in parallel with elevated enzyme activity; however, the authors did not specify which rosacea subtype had been assessed. In our study, we could not detect significantly elevated levels of KLK5 mRNA in PPR, but we did not perform protein level assays or enzyme activity measurements. Among AMPs, only the expression of cathelicidin was assessed previously in PPR, whereas data regarding hBD-2 is available only in ocular rosacea. In line with these previous results, in our study, cathelicidin and hBD-2 were significantly upregulated in PPR as compared with SGP skin at the mRNA level.

In conclusion, our detailed molecular biological study, including whole transcriptome and bioinformatic analyses, as well as QRT-PCR and quantitative IHC studies, found that in PPR all major components of the skin permeability barrier is severely damaged, which may contribute significantly to the pathophysiology of the disease. Studying barrier alterations has become of great importance in recent years. In AD, it has been proven that barrier disruption is able to induce skin inflammation, and, in this manner, can be considered as an initiator of disease pathogenesis. From this point of view, it is quite interesting that we could detect highly similar barrier alterations in PPR and AD. Literature data and our own results suggest that the altered expression of CE components, desmosome and TJ molecules, as well as

alarmin barriers and AMPs, indeed show similarities in the two diseases. These similarities were confirmed at the protein level by IF staining of certain molecules. The demonstrated similarity between the barrier disruptions in PPR and AD is surprising because, up until now, mainly the differences in clinical features and immune composition of these diseases have been highlighted. It is well known that barrier damage in AD can be an initiator of the inflammation that characterizes the disease, but our results did not allow us to determine whether barrier damage in rosacea is an initiator or a consequence of inflammation. Barrier damage may occur because of the Th1/Th17 type inflammation that is characteristic in rosacea, and IL-17A recently has been shown to downregulate FLG, LOR, and KRT10 mRNA levels in organotypic three-dimensional skin equivalents. On the other hand, it is also possible that the dysfunctional barrier is the initiating factor of rosacea development. Although barrier alteration is an adjuvant factor for Th2 type inflammation in AD, the reason why similar barrier disruption may precipitate Th1/Th17 type inflammation in rosacea could be that AD has an SGP region preference, whereas rosacea localizes exclusively on SGR skin. SGR and SGP skin areas have prominently different homeostatic immune and barrier characteristics. Whereas SGR skin regions dispose significantly higher AMP levels, noninflammatory Th17( $\beta$ ) and regulatory T-cell counts, and constitutive expression of homeostatic short form thymic stromal lymphopoietin (sfTSLP), SGP skin is characterized by low AMP levels and T-cell counts, without TSLP presence under steady-state. These features of the skin seem to be very similar to that of another barrier, namely the gut, where the regional immune-related differences are well known. Th17( $\beta$ ) cells are enriched and sfTSLP is expressed in the small intestine, in contrast to the colon, where Th17( $\beta$ ) cells are absent and sfTSLP is present only in the proximal part. It has been hypothesized that these unique immune and barrier characteristics of different sections of the gut may lead to different types of immune-mediated diseases. In Crohn's disease, the loss of sfTSLP from the small intestine can promote the activation of inflammatory Th1/Th17 cells, whereas in ulcerative colitis, significantly increased inflammatory long form TSLP levels initiate Th2 type inflammation in the colon. Based on these findings, it is hypothesized that similar barrier alterations in the SGR and GP skin regions, because of their different homeostatic immune and barrier milieu, initiate distinct immune-mediated skin diseases with unique clinical features driven by different Th subsets (AD on SGP and PPR on SGR areas). Notably, De Benedetto et al. already raised the possibility that barrier defects can lead to the production of keratinocyte-derived mediators including pro-Th2 and pro-Th17 types that affect the characteristics of Th response. To determine if PPR barrier damage is the initiator of the disease or a consequence

of manifested inflammation, the exact time of barrier disruption should be studied and a detailed analysis of the perilesional and/or nonlesional skin of patients with PPR should be performed in the future. Moreover, analogous experiments are needed in other subtypes of rosacea. In summary, our results unambiguously prove the presence of severe barrier alterations in the facial skin of patients with PPR; thus, we suggest that skin barrier restoring therapies should be incorporated into clinical guidelines for rosacea management, similar to that of AD.

## SUMMARY

As a first step, in order to study barrier function, we performed a transepidermal water loss (TEWL) measurement in the healthy sebaceous gland-rich (SGR), apocrine gland-rich (AGR) and gland-poor (GP) skin regions. We found significantly higher TEWL levels in the SGR and AGR regions compared to GP areas, which indicates that AGR and SGR regions may have impaired barrier function. Thus, we investigated the most important permeability barrier related molecules in different skin regions by gene and protein level studies: cornified envelope (CE) molecules (KRT1, KRT10, LCE1D, LCE1F, SPRR1A, SPRR2A, TGM1 and TGM5), desquamation (KLK5, KLK7), the ABCA12 lipid transporter molecule, the (corneo) desmosome (CDH1, CDSN, DSC1, DSG1, PKP1) and tight junction components (CLD1, CLDN16, OCLN). Our investigations were performed by QRT-PCR, IHC and IF and the distribution of junction structures were visualized using confocal microscopy. According to our findings, higher TEWL and KLK levels were detected in the SGR/AGR skin areas, although the expression of (corneo)desmosome and TJ proteins were decreased in these regions. In addition, we also detected irregularly distributed (corneo)desmosomes and TJs in the SGR and AGR skin areas compared to GP skin. In summary, we found that SGR and AGR areas are characterized by weaker permeability barrier features compared to GP skin regions.

In our second study, using several molecular biology methods, we aimed to investigate the permeability barrier alterations in skin samples from patients with rosacea (PPR), and compared them to healthy SGR skin. In this study, transcriptome analysis and bioinformatics analyses were performed. Validation of the expression levels were performed by QRT-PCR, IHC and IF methods. Based on our findings, the proliferation markers (KRT6, 16, 17) showed significantly higher expression levels in PPR, while molecules taking part in differentiation (FLG, LCE1, LOR, KRT1, 10) and cell junction formation (CLDN1, 16, 23, CDH1, CDSN, DSC1, DSG1, PKP1) were significantly downregulated compared to SGR skin. In conclusion, all major components of the permeability barrier in PPR are severely impaired, which may significantly contribute to disease pathophysiology. In atopic dermatitis, it is known that barrier alteration induces skin inflammation and can be considered as an initiating factor in the pathogenesis of the disease, which is interesting since in our current study we detected very similar barrier alterations in PPR.

## PUBLICATION LIST



**UNIVERSITY of  
DEBRECEN**

**UNIVERSITY AND NATIONAL LIBRARY  
UNIVERSITY OF DEBRECEN**

H-4002 Egyetem tér 1, Debrecen  
Phone: +3652/410-443, email: publikaciok@lib.unideb.hu

Registry number: DEENK/456/2022.PL  
Subject: PhD Publication List

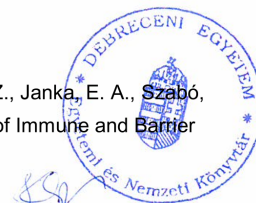
Candidate: Barbara Retzlerné Medgyesi  
Doctoral School: Gyula Petrányi Doctoral School of Allergy and Clinical Immunology  
MTMT ID: 10083376

### List of publications related to the dissertation

1. Kapitány, A., **Retzlerné Medgyesi, B.**, Jenei, A., Somogyi, O., Szabó, L., Gáspár, K., Méhes, G., Hendrik, Z., Dócs, K., Szűcs, P., Dajnoki, Z., Szegedi, A.: Regional Differences in the Permeability Barrier of the Skin: implications in Acantholytic Skin Diseases.  
*Int. J. Mol. Sci.* 22 (19), 1-15, 2021.  
DOI: <http://dx.doi.org/10.3390/ijms221910428>  
IF: 6.208
2. **Retzlerné Medgyesi, B.**, Dajnoki, Z., Béke, G., Gáspár, K., Szabó, I. L., Janka, E. A., Pólska, S., Hendrik, Z., Méhes, G., Töröcsik, D., Bíró, T., Kapitány, A., Szegedi, A.: Rosacea is Characterized by a Profoundly Diminished Skin Barrier.  
*J. Invest. Dermatol.* 140 (10), 1938-1950, 2020.  
IF: 8.551

### List of other publications

3. Dajnoki, Z., Somogyi, O., **Retzlerné Medgyesi, B.**, Jenei, A., Szabó, L., Gáspár, K., Hendrik, Z., Gergely, P., Imre, D., Pólska, S., Töröcsik, D., Zouboulis, C. C., Prens, E. P., Kapitány, A., Szegedi, A.: Primary alterations during the development of hidradenitis suppurativa.  
*J. Eur. Acad. Dermatol. Venereol.* 36 (3), 462-471, 2022.  
DOI: <http://dx.doi.org/10.1111/jdv.17779>  
IF: 9.228 (2021)
4. Gáspár, K., Jenei, A., Khasawneh, A., **Retzlerné Medgyesi, B.**, Dajnoki, Z., Janka, E. A., Szabó, I. L., Hendrik, Z., Méhes, G., Szegedi, A., Kapitány, A.: Comparison of Immune and Barrier Characteristics in Scalp and Skin Psoriasis.  
*Acta Derm.-Venereol.* 100 (14), 1-7, 2020.  
DOI: <https://doi.org/10.2340/00015555-3553>  
IF: 4.437





5. Jenei, A., Dajnoki, Z., **Retzlerné Medgyesi, B.**, Gáspár, K., Béke, G., Kinyó, Á., Méhes, G., Hendrik, Z., Dinya, T., Töröcsik, D., Zouboulis, C. C., Prens, E. P., Bíró, T., Szegedi, A., Kapitány, A.: Apocrine Gland-Rich Skin Has a Non-Inflammatory IL-17-Related Immune Milieu, that Turns to Inflammatory IL-17-Mediated Disease in Hidradenitis Suppurativa. *J. Invest. Dermatol.* 139 (4), 964-968, 2019.  
DOI: <http://dx.doi.org/10.1016/j.jid.2018.10.020>  
IF: 7.143
6. Béke, G., Dajnoki, Z., Kapitány, A., Gáspár, K., **Retzlerné Medgyesi, B.**, Pólska, S., Hendrik, Z., Péter, Z., Töröcsik, D., Bíró, T., Szegedi, A.: Immunotopographical Differences of Human Skin. *Front. Immunol.* 9, 1-15, 2018.  
DOI: <http://dx.doi.org/10.3389/fimmu.2018.00424>  
IF: 4.716
7. Khasawneh, A., Baráth, S., **Retzlerné Medgyesi, B.**, Béke, G., Dajnoki, Z., Gáspár, K., Jenei, A., Pogácsás, L., Pázmándi, K. L., Gaál, J., Bácsi, A., Szegedi, A., Kapitány, A.: Myeloid but not plasmacytoid blood DCs possess Th1 polarizing and Th1/Th17 recruiting capacity in psoriasis. *Immunol. Lett.* 189, 109-113, 2017.  
DOI: <http://dx.doi.org/10.1016/j.imlet.2017.04.005>  
IF: 2.436

**Total IF of journals (all publications): 42,719**

**Total IF of journals (publications related to the dissertation): 14,759**

The Candidate's publication data submitted to the iDEa Tudóstér have been validated by DEENK on the basis of the Journal Citation Report (Impact Factor) database.

20 October, 2022

